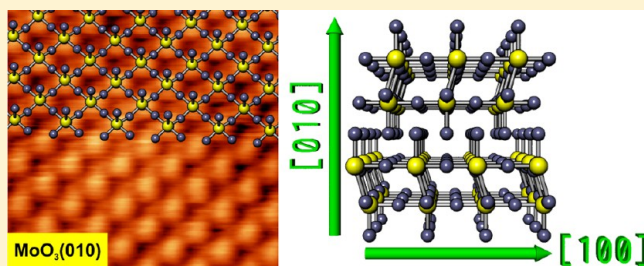


Well-Ordered Molybdenum Oxide Layers on Au(111): Preparation and Properties

S. Guimond,^{†,§} D. Göbke,^{†,||} J. M. Sturm,^{†,⊥} Y. Romanyshyn,[†] H. Kuhlenbeck,^{*,†} M. Cavalleri,^{‡,#} and H.-J. Freund[†]

[†]Chemical Physics Department and [‡]Theory Department, Fritz Haber Institute of the Max Planck Society, Faradayweg 4-6, 14195 Berlin, Germany

ABSTRACT: MoO₃ layers on Au(111) were prepared via oxidation of molybdenum at elevated temperature in an atmosphere of 50 mbar of O₂. Three different types of oxide structures were identified. Up to monolayer oxide coverage a structure with a $c(4 \times 2)$ unit cell relative to the Au(111) unit cell forms. This structure was previously identified as being similar to a monolayer of α -MoO₃.¹ At larger coverages of up to two layers an oxide with a $11.6 \text{ \AA} \times 5 \text{ \AA}$ rectangular unit cell appears. Further increase in the coverage leads to the occurrence of crystallites of regular α -MoO₃ with a very small density of defects. These crystallites grow with the (010) plane parallel to the substrate surface and with random azimuthal orientation leading to rings in the LEED pattern. With increasing layer thickness the crystallites start to coalesce until finally a closed film forms. These layers sublime at temperatures between about 670 and 770 K with the MoO₃ aggregates sublimating at lower temperature than the bilayer and monolayer films.



INTRODUCTION

Recently we reported about the preparation and the properties of well-ordered V₂O₅(001) layers on Au(111),² which we supplement here by an investigation of molybdenum trioxide layers on Au(111). Molybdenum trioxide is the compound with the highest Mo oxidation state in the Mo–O system. Like V₂O₅, MoO₃ is an oxide of high industrial relevance. Molybdenum trioxide is extensively used as a key component in mixed oxide catalysts. (See, for instance, refs 3 and 4.) Good examples are iron-molybdate catalysts, which are industrially used (besides, or in combination with silver-based catalysts) for the selective oxidation of methanol to formaldehyde.⁴ Formaldehyde is a very important building block for the chemical industry (for instance, for the production of thermosetting resins). Important questions regarding the nature of the active sites and the reaction mechanisms at the surface of iron-molybdate catalysts are not clearly answered yet. However, much evidence indicates that Mo plays the major role in the relevant catalytic reactions.⁴ This is partially substantiated by the observation that MoO₃ alone shows a rather good activity for several reactions, including the oxidation of methanol to formaldehyde⁵ and the partial oxidation of propene.⁶

The most common polymorph of MoO₃ is the orthorhombic α -phase³ with unit cell parameters $a = 3.9628 \text{ \AA}$, $b = 13.855 \text{ \AA}$, and $c = 3.6964 \text{ \AA}$.⁷ A monoclinic β -phase was observed at high pressure,³ but this polymorph is rather uncommon and will not be described here. The atomistic structure of α -MoO₃ is depicted in Figure 1. It consists of weakly interacting bilayer sheets that are aligned parallel to the (010) plane. Each bilayer comprises two interleaved planes of corner-sharing MoO₆

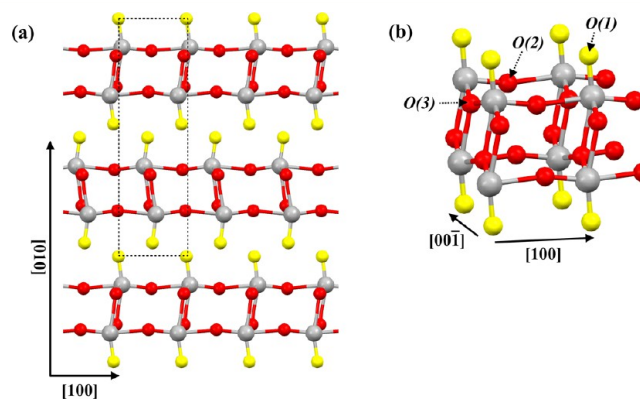


Figure 1. Geometric structure of α -MoO₃.⁷ (a) Stacking of the double layers seen along [001]. (b) Magnified and tilted view showing the structural details in a double layer. Gray spheres indicate the position of the molybdenum atoms while yellow and red spheres pertain to oxygen atoms (yellow indicating molybdenyl O atoms). The unit cell is indicated in panel a, and the nonequivalent oxygen centers, O(1, 2, 3), are labeled in panel b.

octahedra. The octahedra of two adjacent planes share edges. The octahedral MoO₆ building unit is severely distorted, and the metal–oxygen bond lengths vary between 1.68 and 2.33 Å. As indicated in Figure 1b, α -MoO₃ contains three structurally different oxygen sites:^{3,8,9} terminal oxygen coordinated to only

Received: November 18, 2012

Revised: April 8, 2013

Published: April 10, 2013

one Mo center (O1) and bridging oxygen atoms coordinated to two (O2) or three (O3) Mo centers. The interatomic bonds in MoO₃ have both ionic and sizable covalent contributions.^{3,9} The calculated Mo charge (between 2.23+⁹ and 2.59+⁸, depending on the calculation methodology) is much smaller than the formal charge expected for pure ionic bonds (6+). Since the adjacent bilayers along [010] are linked only by weak van der Waals forces, (010) is a natural cleavage plane of α -MoO₃. Like for V₂O₅, the catalytic activity of MoO₃ is often described by a redox mechanism of the Mars–van Krevelen type,¹⁰ where the catalyst acts as a renewable oxygen source. Here the relatively open crystal structures most probably play a crucial role for the diffusion of oxygen, both from the bulk volume to the surface to annihilate vacancies and from the surface to the bulk to replenish the overall O content.

Triggered by the catalytic activity of molybdenum oxides, we started to investigate the preparation and the structural, electronic, and thermal properties of ordered MoO₃ layers on Au(111) to establish a well-characterized substrate for model catalytic studies. In such studies, the chemical action of molecules on surfaces is investigated for simple, often single-crystalline substrates, which may also be modified in well-defined ways. In most cases the studies are performed under low-pressure conditions that permit to apply experimental techniques, which cannot easily be applied to real catalysts under working conditions. The first steps of such an investigation are the preparation of such layers and the study of their properties.

The use of thin layers often has advantages over the use of single crystals. One advantage in the case of MoO₃ layers is that they can easily be prepared in situ, which is important for experiments that damage the surface like surface reaction studies. Another relevant aspect is that experimental methods that require that the sample is conductive cannot be applied to nonconductive single crystals, whereas they can be applied to thin layers if they are not too thick. Finally, in some cases, like the one of MoO₃, it is possible to prepare high-quality layers of an oxide, where sufficiently large high-quality single crystals are not available.

The formation of molybdenum trioxide thin films was investigated for a broad range of deposition methods, including thermal evaporation of MoO₃,^{11,12} reactive pulsed laser deposition,¹³ spin coating using peroxy-molybdic precursors,¹⁴ and hot filament metal oxide deposition.¹⁵ Most of these studies were focused onto the growth of micrometer- or sub-micrometer-thick MoO₃ films suitable for intercalation devices (e.g., microbatteries or electrochromic applications), where the precise control of the surface structure does not play a crucial role or at least was not considered to be very important. Reports reveal that MoO₃ thin films deposited at low substrate temperatures ($T < 373$ K) are usually amorphous. In these cases, postdeposition annealing in an O₂ atmosphere at $T > 523$ K was necessary to crystallize the films. Julien et al.¹¹ and Gaigneaux et al.¹⁴ reported that the crystallites obtained after annealing preferentially expose (010) basal faces, which are mainly aligned parallel to the substrate surface. Unfortunately, the characterization of the films in the above-mentioned studies was almost always carried-out ex situ and involved exposure of the sample to air prior to (or during) the analysis that can change the oxygen content and contaminate the sample. We prepared and studied the Mo oxide layers in the same machine so that it was not required to expose the prepared layers to air.

The oxidation of bulk molybdenum under UHV-compatible O₂ pressures ($<10^{-4}$ to 10^{-3} mbar) rather typically results in the formation of MoO₂ surface layers.^{16–19} The presence of higher oxidation states is also sometimes reported after extensive annealing in O₂, but these species (perhaps polymolybdates) are disordered and exist in rather small quantities.^{16,17} Indeed, it is believed that MoO₃ desorbs after it is formed under UHV-compatible oxidation conditions because the necessary oxidation temperature is higher than the temperature at which MoO₃ sublimates.¹⁶ Bourgeois, Domenichini, and coworkers investigated the oxidation of very thin layers of Mo deposited on TiO₂ (110) by postdeposition annealing in UHV. (See ref 20 and references therein.) This work shows that the Mo atoms reduce the TiO₂ substrate to form MoO₂ thin films or clusters. If the annealing process is carried out at higher temperature, then MoO₃ forms and sublimates. Under these circumstances it appeared that fast oxidation in a high-pressure cell as successfully done for the preparation of V₂O₅ thin films² could also be appropriate for the preparation of MoO₃ thin films. Similar to the investigations performed for V₂O₅(001),² various amounts of Mo were oxidized to study the formation of MoO₃ films with different thicknesses.

We found that the MoO₃ thin films grow with [010] orientation, as also observed by Julien et al.¹¹ and Gaigneaux et al.¹⁴ This is not surprising because the (010) surface has a small surface energy that is related to the weak interaction between the MoO₃ bilayers.

Au(111) was chosen as substrate because gold is rather inert, which permits us to perform studies at elevated pressures. Another advantage of the inertness of gold is that the interaction with overlayers is usually rather weak. One may expect that this is especially the case for MoO₃(010) due to the small surface energy. This is an important aspect because it may result in a reduced lattice strain at the interface between the Au(111) and MoO₃(010) lattices. Therefore, we felt that there might be a good chance that well-ordered MoO₃(010) layers grow despite the Au(111)–MoO₃(010) lattice misfit.

■ EXPERIMENTAL SECTION

Room-temperature STM images were acquired in a system equipped with facilities for STM (Omicron STM 1), XPS, and TPD. Sample heating was performed with a tungsten filament that was mounted behind the sample. It could be used for heating via electron irradiation or via heat radiation in the case that no voltage was applied between the filament and the sample. Cooling was possible via a flexible copper braid fixed to the sample holder plate on one side and to a liquid nitrogen evaporator on the other side. With this setup, temperatures as low as ~ 100 K could be reached. The temperature was measured with a chromel–alumel thermocouple pressed with a metal sheet into a slit in the side of the sample.

For TPD measurements, the sample was placed at a distance of 0.5 mm in front of the nozzle of the pumped housing (“Feulner cup”, see ref 21) of a quadrupole mass spectrometer (Hiden HAL RC 201). Spectra were recorded with a heating rate of 0.5 K/s using a feedback temperature controller (Schlichting Instruments).

Core-level XPS spectra were recorded with a laboratory X-ray source employing Mg K α radiation and detection with an Omicron EA125 electron analyzer, whereas valence band spectra were measured with light from the UE52 monochromator at the BESSY II electron storage ring in Berlin using

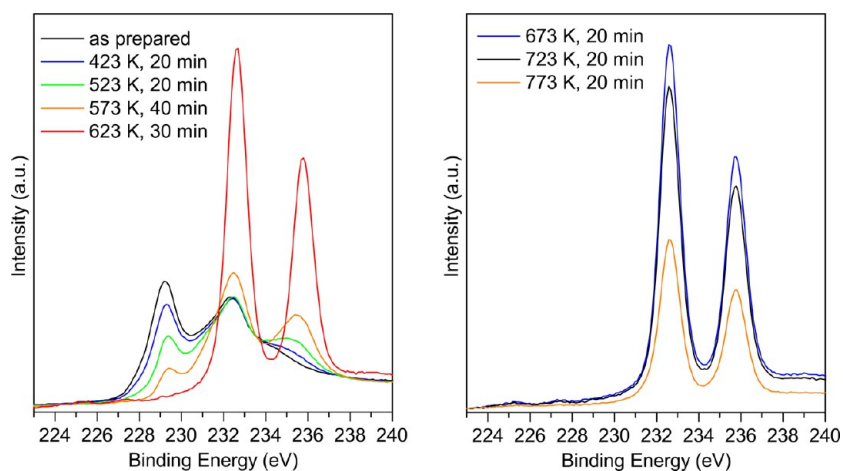


Figure 2. Mo3d XPS spectra of a MoO_x film obtained after annealing at different temperatures in 50 mbar of O₂. The film, which was oxidized in the high-pressure cell, was prepared by evaporation of 45 Å of Mo in an atmosphere of 5×10^{-6} mbar of O₂. High-pressure oxidation of metallic molybdenum layers yields similar results. For all spectra, the XPS intensity was normalized to the background intensity at 210 eV. Mg K α radiation was employed to excite the electrons and the detector was set to detect electrons in a cone along the surface normal.

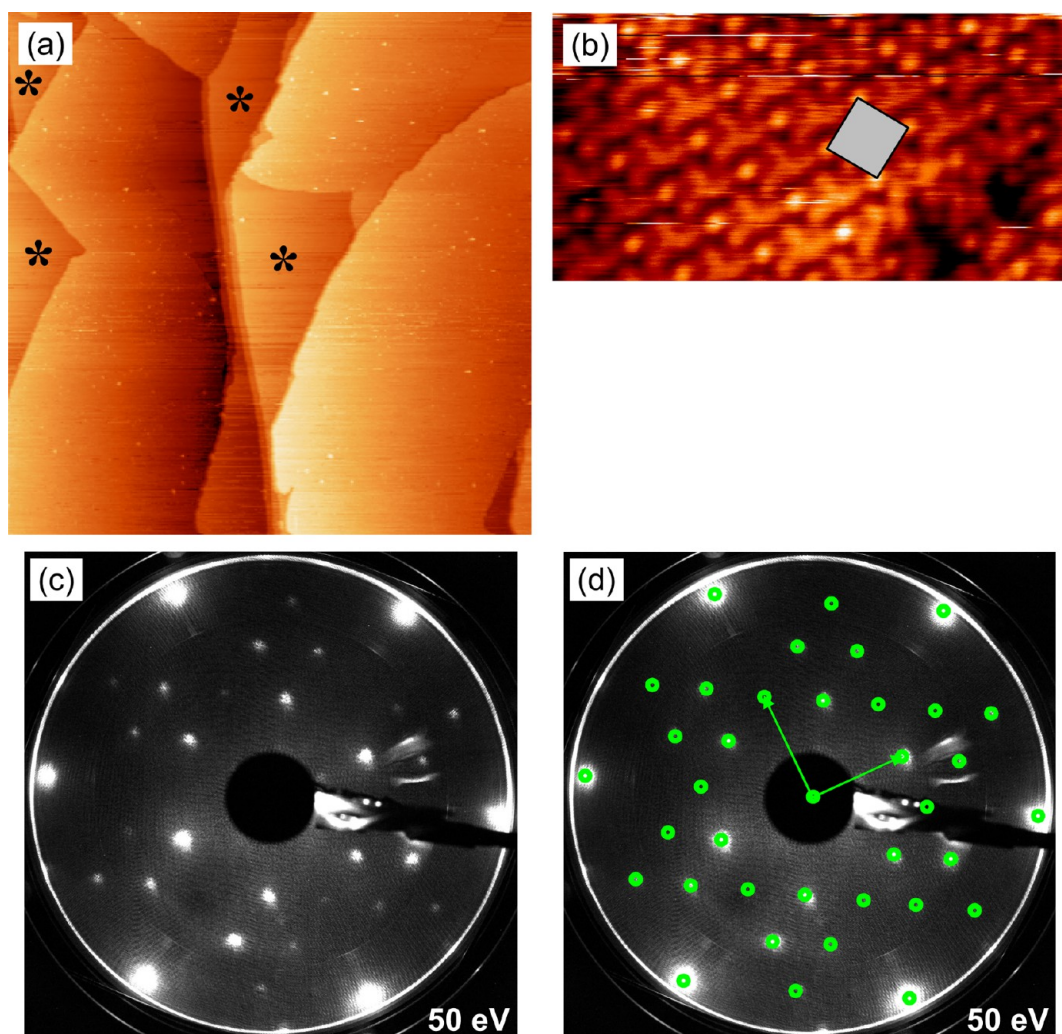


Figure 3. STM images [(a) 300 nm \times 300 nm, 2.5 V, 0.2 nA; (b) 5 nm \times 2.56 nm, 2.5 V, 0.2 nA] and LEED pattern (c) obtained after annealing 0.46 MLE Mo/Au(111) in 50 mbar O₂ at 673 K for 10 min. (d) Reproduction of the LEED pattern using a 5.77 Å \times 5 Å rectangular unit cell and taking into account the substrate three-fold symmetry. (The bright spots at the border of the screen are the first-order Au(111) spots.) Exposed Au(111) areas are marked with * in panel a.

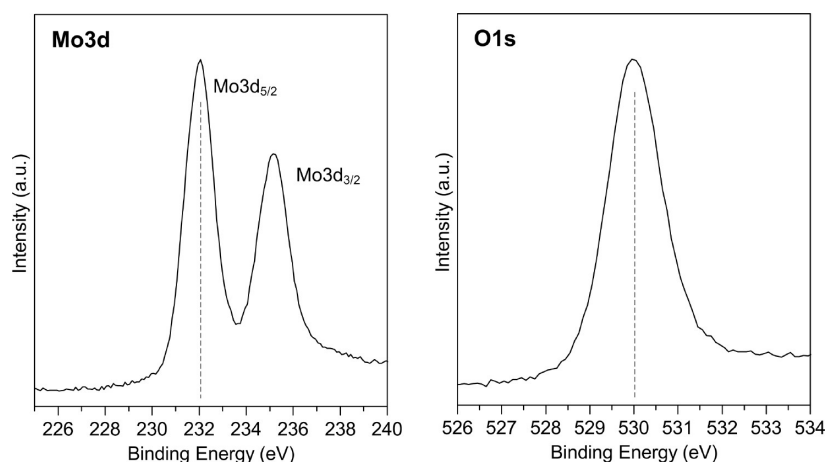


Figure 4. Mo3d and O1s XPS spectra of a $c(4 \times 2)$ Mo oxide monolayer obtained after annealing 0.46 MLE Mo/Au(111) in 50 mbar O_2 at 673 K for 10 min. Mg $K\alpha$ radiation was employed to excite the electrons, and the detector was set to detect electrons in a cone along the surface normal.

a Scienta SES 200 hemispherical electron energy analyzer for electron detection. NEXAFS data were acquired in the same end station, as used for the valence band spectra. Part of the NEXAFS spectra was recorded with a partial yield detector, essentially consisting of a channeltron with two grids mounted in front of its entrance opening. The grid nearer to the channeltron opening was set to a voltage of -60 V to reflect low-energy electrons, and the other grid was set to ground potential. Another part of the NEXAFS spectra was measured in the total yield mode, where the current flowing from ground to the sample is recorded as a function of the photon energy. Intensity normalization of NEXAFS spectra of the oxide-covered surfaces was achieved by dividing by a spectrum of the noncovered surface, which does not exhibit structured intensity in the investigated energy range.

The films were prepared by oxidation of a Mo layer on Au(111) in a high-pressure cell (see ref 2) attached to the UHV chamber. Mo was evaporated with an Omicron EFM3 e-beam evaporator at a rate of ~ 0.4 Å/min (0.2 MLE/min) while the substrate was held at room temperature. Mo layer thicknesses are given in monolayer equivalents (MLEs), where 1 MLE corresponds to one Mo atom per Au(111) gold surface atom ($\sim 1.39 \times 10^{15}$ atoms/cm²). The Mo layers were oxidized by heating the sample in a stream of flowing oxygen at a constant pressure of 50 mbar in the high-pressure cell. At the end of the oxidation procedure, the heating was switched off and the sample was cooled in the oxygen stream. The high-pressure cell was evacuated after the sample has reached a temperature of 373 K, and the sample was transferred back into the main chamber. No traces of surface contamination could be detected with XPS on the oxide surface.

RESULTS AND DISCUSSION

Initial experiments were done to find a suitable oxidation temperature/time combination for the preparation of completely oxidized MoO_3 layers. Some of the results are summarized in Figure 2. The graphs show a series of Mo3d XPS spectra obtained for a rather thick film annealed in the high-pressure cell at different temperatures in 50 mbar of O_2 . The annealing steps were done sequentially, starting at 423 K and going up to 773 K. The Mo3d spectrum of the as-prepared layer is displayed in black in the left panel of Figure 2. It exhibits two distinct peaks at 229.2 and 232.3 eV, which roughly correspond to the binding energies of the $Mo3d_{5/2}$ and

$Mo3d_{3/2}$ levels of MoO_2 , respectively.^{18,22} The shoulder at ~ 234.4 eV reveals the presence of a species with a higher oxidation state. These observations correspond well to the findings of other groups for the oxidation of Mo under oxygen partial pressures in the 10^{-6} mbar range.^{16,17}

The intensity of the Mo^{6+} levels gradually increases with increasing annealing temperature until at ~ 623 K a peak structure characteristic of pure MoO_3 , with a $Mo3d_{5/2}$ binding energy of ~ 232.65 eV and a spin-orbit splitting of ~ 3.2 eV,²² shows up. Thus an annealing temperature of at least 623 K is required to fully oxidize the Mo film. Annealing at 673 K leads to an essentially identical spectrum while some Mo3d intensity was lost after annealing at 723 K and a drastic decrease in the peak area was observed after annealing at 773 K. This shows that sublimation of the MoO_3 film sets in at ~ 723 K. This conclusion is supported by the TPD data presented below and agrees well with results reported in the literature.²³ In light of these results, an annealing temperature of 673 K was used for most of the preparations. This makes sure that the film is fully oxidized (for the Mo thicknesses used here) and avoids significant material loss due to sublimation.

Similar to the case of V_2O_5 on Au(111),² α - MoO_3 was obtained only for thicker films, whereas the oxidation of small amounts of Mo led to the formation of well-ordered overlayers with structures that do not correspond to any known bulk molybdenum oxide. These Au(111)-specific layers are discussed first, followed by a description of the thicker films with α - MoO_3 structure and a discussion on the thermal stability of the films under UHV conditions.

Structure of the First Layers. The oxidation of molybdenum deposits with an equivalent layer thickness of up to ~ 0.5 MLE in 50 mbar of O_2 at 673 K resulted in the formation of flat oxide films with a $c(4 \times 2)$ unit cell. STM and LEED results of a film prepared by oxidation of 0.46 MLE Mo are shown in Figure 3. The large area (300 nm \times 300 nm) STM image shown in Figure 3a clearly indicates that the oxide forms a smooth, uniform film on the Au(111) substrate. Areas where the substrate surface is still exposed are marked with an asterisk on the picture. These areas appear smoother and they are easily identified by the Au(111) herringbone reconstruction zigzag pattern at higher resolution. Most of the substrate is covered by the film (also seen in other images taken at various places on the sample surface). High-resolution STM pictures like the one shown in Figure 3b reveal a well-ordered structure

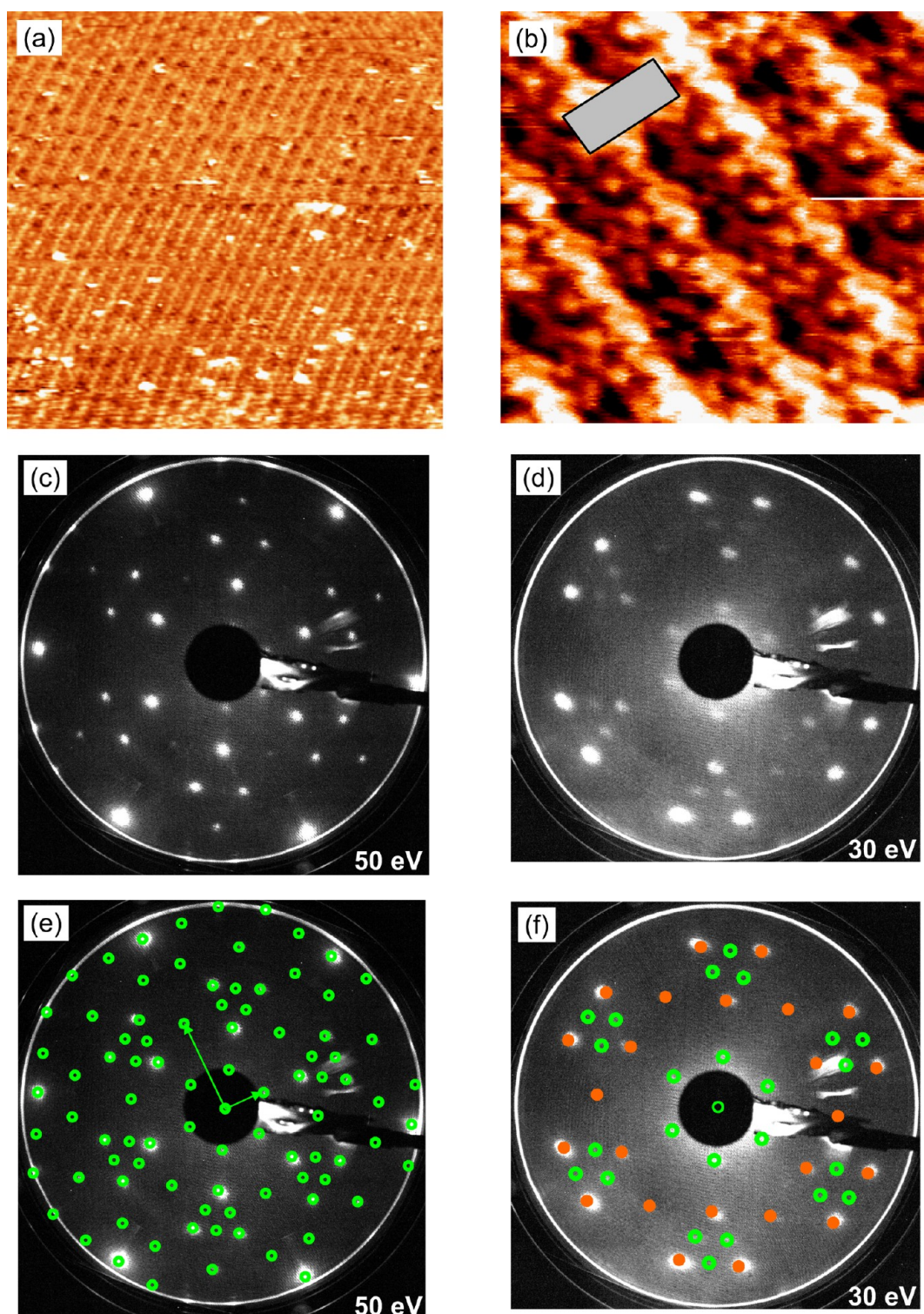


Figure 5. STM images [(a) 27 nm \times 26.7 nm, 2.5 V, 0.2 nA; (b) 4.1 nm \times 4.1 nm, 2.5 V, 0.2 nA] and LEED patterns (c,d) obtained after annealing 0.92 MLE Mo/Au(111) in 50 mbar O₂ at 673 K for 10 min. (e,f) Reproduction of the LEED patterns shown in panels c and d using a 11.6 Å \times 5 Å rectangular unit cell and taking into account the substrate's three-fold symmetry.

with a 5.8 Å \times 5 Å rectangular unit cell (indicated by the gray rectangle in the image). Only a limited number of point defects could be observed with STM. The sharpness of the spots in the LEED pattern shown in Figure 3c indicates that the film must have a rather good long-range order. The spots in the LEED pattern correspond to three rotational domains of a $c(4 \times 2)$ overlayer (in matrix notation this is a (2,1|0,2) superstructure),

which has a 5.77 Å \times 5 Å rectangular unit cell, as observed with STM. The absence of the (01) first-order LEED spots that appear for nonvertical incidence of the electron beam points toward the existence of a glide plane in the structure.²⁴

The same $c(4 \times 2)$ LEED pattern has been observed by Biener and coworkers after the oxidation of Mo nanoclusters on Au(111) (deposited either by CVD of Mo(CO)₆ or Mo

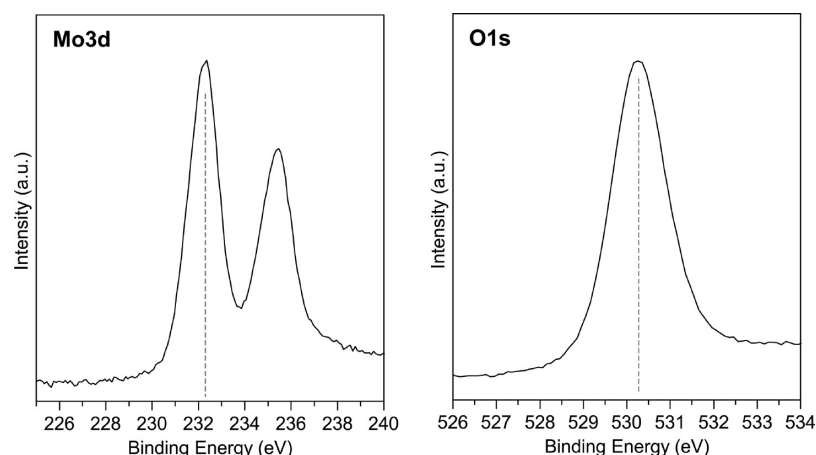


Figure 6. Mo3d and O1s XPS spectra of a film obtained after annealing 0.92 MLE Mo/Au(111) in 50 mbar O₂ at 673 K for 10 min. Mg K α radiation was employed to excite the electrons and the detector was set to detect electrons in a cone along the surface normal.

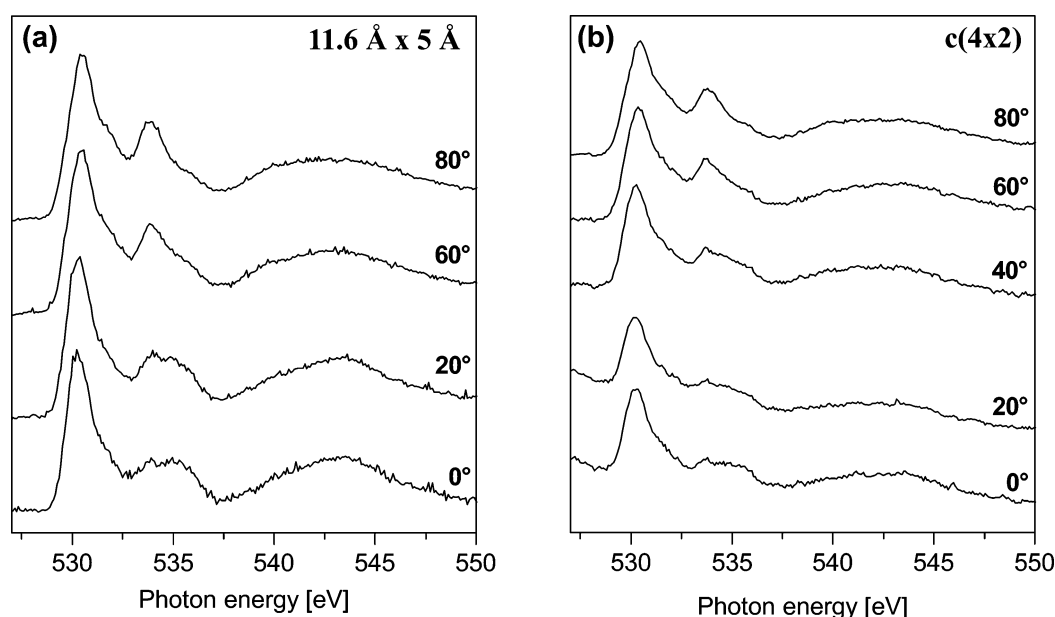


Figure 7. Angle-resolved O1s NEXAFS spectra (O K-edge) of (a) a film with a 11.6 Å \times 5 Å rectangular surface unit cell and (b) a $c(4 \times 2)$ monolayer. The layers were prepared by oxidation of 0.92 MLE Mo/Au(111) in 50 mbar O₂ at 673 and 773 K, respectively. Annealing at 773 K yields a monolayer-thick $c(4 \times 2)$ film because the second layer sublimates at 773 K. In both cases, the polar incidence angle of the photon beam was varied between 0 and 80°, with 0° being along the surface normal. The spectra were recorded using partial yield detection.

evaporation) with NO₂.^{1,25} This structure was investigated in detail and an atomistic model was proposed based on DFT calculations.²⁶ According to this publication, the film is essentially a distorted α -MoO₃ monolayer with bond distances and angles that are somewhat modified to fit the Au lattice.

The Mo surface atom density in the $c(4 \times 2)$ monolayer is $\sim 0.7 \times 10^{15}$ atoms/cm², which means that an initial Mo coverage of ~ 0.5 MLE is required to obtain a full monolayer. Large-area STM images obtained after oxidation of 0.46 MLE Mo (Figure 3a) indeed show that most of the substrate is covered by the oxide monolayer. The size of the free areas in Figure 3a could point toward a slightly lower Mo metal coverage than expected from the evaporation rate calibration. Also, the sublimation of a small amount of material during the oxidation cannot be completely ruled out.

Mo3d and O1s XPS spectra of the $c(4 \times 2)$ oxide monolayer are shown in Figure 4. The Mo3d_{5/2} and O1s peaks appear at binding energies of 232 and 530 eV, respectively, which is ~ 0.7

eV below values reported for α -MoO₃.²² Like for the V₂O₅ monolayer structures,²⁷ this shift can be attributed to a screening of the XPS final state core holes by the Au(111) electrons. Interestingly, about the same shift is observed for the monolayers of both V₂O₅ and MoO₃. A surface structure with a larger unit cell was observed after oxidation of slightly larger Mo amounts. STM images and LEED patterns obtained after oxidation of 0.92 MLE Mo (673 K, 50 mbar O₂, 10 min) are shown in Figure 5. Corrugation lines are observed in the large-scale STM image shown in panel a. Higher-resolution images, although somewhat noisy, reveal a ~ 11.5 Å \times 5 Å rectangular unit cell. (See Figure 5b). In agreement with this, the LEED patterns can be well-reproduced with this unit cell, which is a (2,1|0,4) superstructure in matrix notation. The short unit cell vector of this surface structure has the same length as the one pertaining to the $c(4 \times 2)$ structure described above (5.77 Å \times 5 Å unit cell), while the long unit cell vector has twice the length. As a result, the LEED patterns display the same reflexes

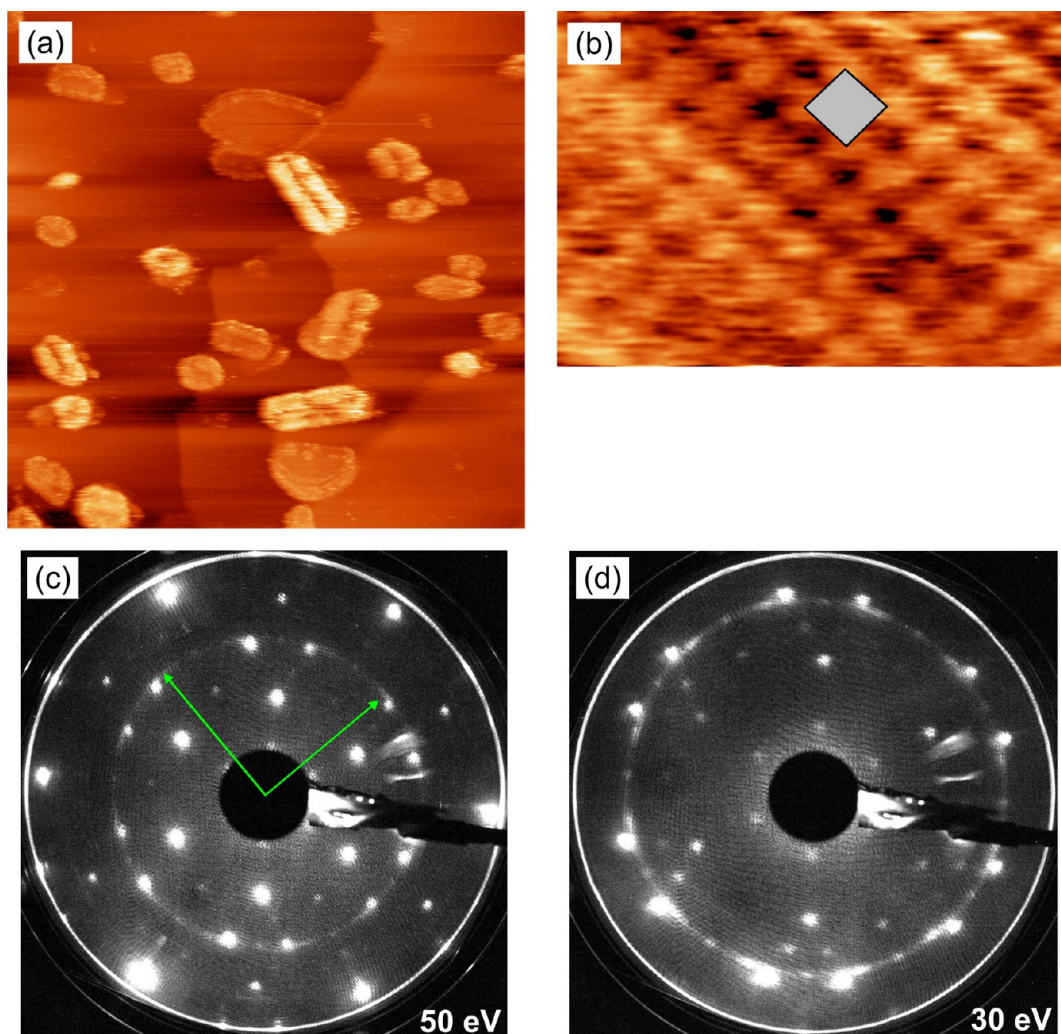


Figure 8. STM images [(a) 300 nm \times 300 nm, 2.5 V, 0.2 nA; (b) 3.2 nm \times 2.2 nm, 2.5 V, 0.2 nA] and LEED patterns (c,d) obtained after annealing 1.15 MLE Mo/Au(111) in 50 mbar O_2 at 673 K for 10 min. Panel b was acquired on one of the brighter areas observed in panel a. The reciprocal space unit cell vectors of $MoO_3(010)$ are shown in panel c.

as those for the $c(4 \times 2)$ structure plus some extra spots. In Figure 5f, the spots that are also observed for the $c(4 \times 2)$ structure are identified with orange circles.

Mo3d and O1s XPS spectra of this film are displayed in Figure 6. The binding energies of both peaks (Mo3d_{5/2}: 232.3 eV, O1s: 530.3 eV) are about 0.4 eV lower than those obtained for α -MoO₃.²² The difference between the XPS spectra of this film and of the $c(4 \times 2)$ monolayer is reminiscent of observations made for the V₂O₅ thin films on Au(111),²⁷ where it was concluded that XPS final state screening by gold electrons is largely limited to the first oxide layer. It may be the case that the same conclusion applies to the thin MoO₃ layers, which would be an indication that the observed 11.6 Å \times 5 Å rectangular unit cell is related to the formation of a second layer of MoO₃. This assumption is supported by the fact that 0.92 MLE of Mo contains about twice the amount of Mo required to complete a full $c(4 \times 2)$ monolayer.

O1s NEXAFS data (O K-edge) were acquired for both the $c(4 \times 2)$ monolayer and the thicker film with a 11.6 Å \times 5 Å rectangular surface unit cell. The spectra are displayed in Figure 7 as a function of the polar incidence angle of the linearly polarized X-ray beam (0° is along the surface normal). The films were prepared in the high-pressure cell by oxidation of

0.92 MLE Mo in 50 mbar of O_2 at a temperature of 673 K for the thicker film and at 773 K for the $c(4 \times 2)$ monolayer. We note that the latter temperature is somewhat above the stability range of the oxide layer. (See the Discussion in the context of Figure 14.) We attribute the successful preparation of the $c(4 \times 2)$ layer at this temperature to a somewhat deviating temperature measurement in the high-pressure cell due to the oxidation of the thermocouple. The energy region between 529 and 537 eV is dominated by two peaks that arise from the excitation of O1s core electrons into unoccupied orbitals with antibonding O2p+Mo4d character.²⁸ The peak at lower energy (maximum at 530.2 eV) can be ascribed to antibonding orbitals, where the O2p admixture points perpendicular to the corresponding O–Mo bond. The other peak at \sim 534 eV refers to orbitals with O2p admixture pointing along the O–Mo bond. The spectra are similar for both thin films to a large extent. In particular, the angular dependence of the various features is well comparable. This points toward rather similar bonding geometries around the Mo centers and similar orientations of the coordination units of both films.

The angular dependence of the intensity of the high energy peak at \sim 534 eV roughly follows the trend observed for MoO₃(010) (discussed later in this text; see also ref 29). O1s

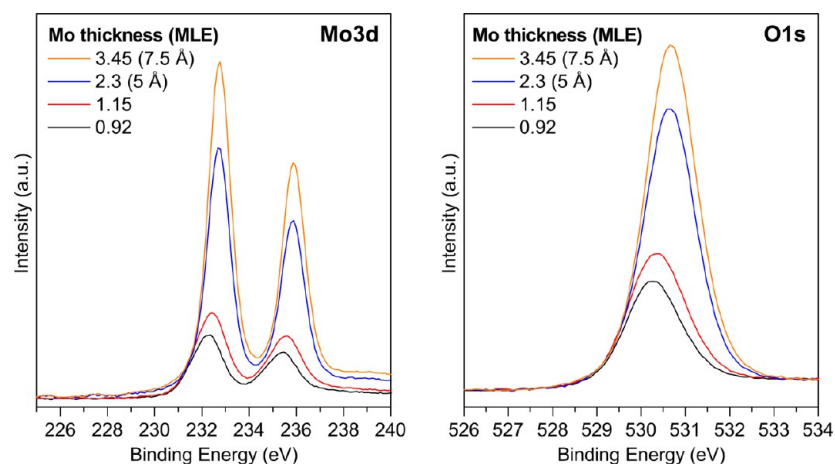


Figure 9. Mo3d and O1s XPS spectra of molybdenum oxide films on Au(111). Mo layers with different thickness were oxidized for 10 min in an atmosphere of 50 mbar O₂ at 673 K. The intensity was normalized to the background intensity at 215 and 525 eV for the Mo3d and O1s spectra, respectively. Mg K α radiation was employed to excite the electrons, and the detector was set to detect electrons in a cone along the surface normal.

NEXAFS spectra of MoO₃(010) were investigated in detail with DFT by Cavalleri et al.²⁸ According to the results of the study, the molybdenyl oxygen atoms are responsible for most of the intensity of the high-energy peak of MoO₃(010) (probably corresponding to the state at \sim 534 eV in the case of the thin films). Because the Mo=O bond is oriented essentially perpendicular to the MoO₃(010) surface normal, the intensity of the high-energy peak (which is related to final state orbitals pointing along the bond) will be highest for grazing photon incidence, that is, when the electric field vector of the X-rays is almost parallel to the surface normal. This describes well the behavior of the peak at \sim 534 eV, thus supporting the idea that both the $c(4 \times 2)$ monolayer and the film with the $11.6 \text{ \AA} \times 5 \text{ \AA}$ surface unit cell contain molybdenyl groups that are oriented at an angle close to the surface normal.

Thicker Films: MoO₃(010). The oxidation of thicker Mo layers leads to the growth of (010)-oriented α -MoO₃ crystallites, which eventually coalesce when the crystallites grow larger. Figure 8 shows STM images and LEED patterns of a film prepared by oxidation of 1.15 MLE Mo. The LEED patterns correspond well to the ones presented in Figure 5 for a film with a $11.6 \text{ \AA} \times 5 \text{ \AA}$ rectangular unit cell, with the addition of faint rings. Two rings with slightly different diameters are visible in the images. The larger one is observed in panel c, whereas the smaller one can be seen in panel d. The radii of the two rings correspond very well to the lengths of the two unit cell vectors of MoO₃(010), as depicted in panel c. The (010) surface of α -MoO₃ does not relax significantly with respect to the bulk structure and it has a $3.7 \text{ \AA} \times 3.96 \text{ \AA}$ rectangular unit cell.^{3,30} (See Figure 1.)

The existence of rings in the LEED patterns can be attributed to azimuthal disorder related to the coexistence of MoO₃(010) domains with random azimuthal orientations. STM results complement this conclusion. The large-scale image in Figure 8a displays a flat film and some crystallites having an apparent height of about 0.7 to 1.3 nm. These crystallites seem to have an extended boundary region with a width of a couple of nanometers, as concluded from the appearance of the islands in the STM image. Higher-resolution images acquired on these crystallites reveal a MoO₃(010) unit cell. (See Figure 8b.) Altogether, these results indicate that MoO₃(010) crystallites start to grow after the completion of the film with a $11.6 \text{ \AA} \times 5 \text{ \AA}$ rectangular surface unit cell, which probably has a thickness

of two oxide monolayers. Thus, for both vanadium pentoxide^{2,27} and molybdenum trioxide the film growth on Au(111) occurs in a Stranski–Krastanov-like mode, where 3D growth starts after the completion of an oxide bilayer with Au(111)-specific structure. In both cases, the 3d crystallites exhibit random azimuthal orientation.

Mo3d and O1s XPS spectra of Mo oxide films with different thickness are compared in Figure 9. The XPS binding energies of the film grown from 1.15 MLE of Mo are higher than those of the bilayer (0.92 MLE Mo), and they are closer to those observed for the thicker films (232.7 and 530.65 eV for the Mo3d_{5/2} and O1s, respectively). Their full width at half-maximum (fwhm, 1.66 eV for Mo3d_{5/2}) is also larger than that observed for both the thinner (0.92 MLE Mo: 1.61 eV for Mo3d_{5/2}) and the thicker films (2.3 MLE Mo: 1.25 eV; 3.45 MLE Mo: 1.2 eV for Mo3d_{5/2}). This is due to the spectral contribution of both the bilayer film and the bulk MoO₃(010) crystallites. As the films get thicker, the contribution of the interface layer is gradually reduced and the XPS peaks shift toward their positions for bulk MoO₃.²²

STM and LEED data of a film prepared by oxidation of 2.3 MLE (\sim 5 Å) Mo are shown in Figure 10. Imaging the film with STM proved to be difficult, and only a few good pictures could be recorded. Strong tip–surface interactions and frequent crashes hampered the scanning process. Nevertheless, some images could be obtained, some of them with good resolution. The film thickness is probably a critical parameter, and one may expect that the investigation of thicker films of stoichiometric MoO₃ will not easily be possible with STM. A similar observation for MoO₃ single crystals was reported by Smith and Rohrer,³⁰ who had to use atomic force microscopy instead of STM. A large-scale image is displayed in Figure 10a. It is rather noisy and suffers from a change of the tip apex in about its middle. One may interpret it such that it displays extended crystallites (\sim 50 nm lateral width) and a few holes with the crystallites exhibiting wide borders similar to the crystallites in Figure 8a. Atomically resolved images acquired on the crystallites (Figure 10b,c) clearly reveal the MoO₃(010) $3.7 \text{ \AA} \times 3.96 \text{ \AA}$ rectangular unit cell. These images also show that the surface of the crystallites has very few point defects.

The rings in the LEED pattern are now more intense than those in Figure 8, which is due to the larger layer thickness. As shown in panel d, the rings can all be related to MoO₃(010)

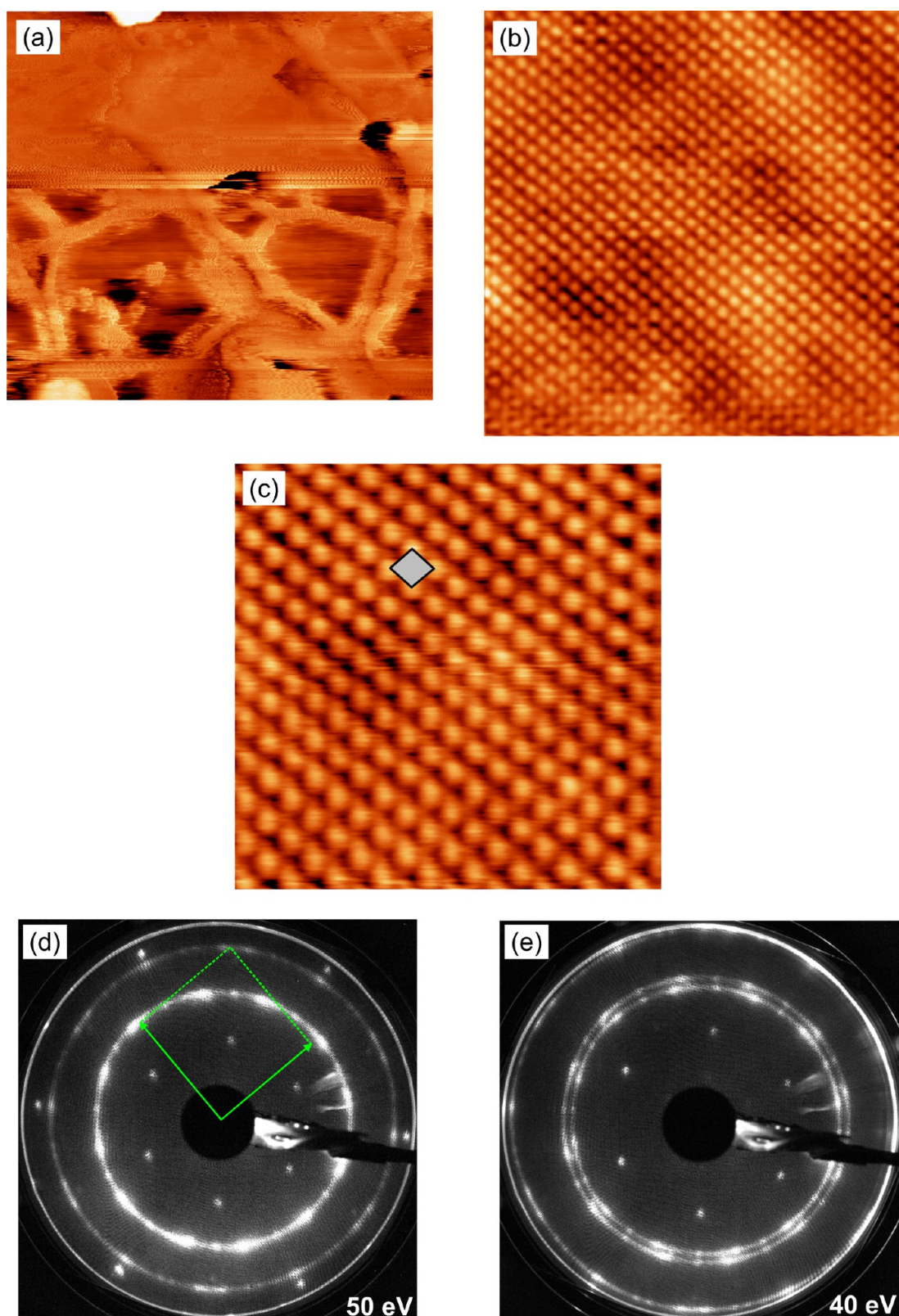


Figure 10. STM images [(a) $300 \text{ nm} \times 274.8 \text{ nm}$, 3 V, 0.7 nA; (b) $10 \text{ nm} \times 10 \text{ nm}$, 2.5 V, 0.7 nA; and (c) $5 \text{ nm} \times 5 \text{ nm}$, 2.5 V, 0.7 nA] and LEED patterns (d,e) obtained after annealing 2.3 MLE Mo/Au(111) in 50 mbar O_2 at 673 K for 10 min. The reciprocal space unit cell vectors of $\text{MoO}_3(010)$ are shown in panel d.

spots that are rotated about the (00) spot. The most intense spots of the bilayer structure can still be detected, which is an indication that some areas of the interface are still exposed. In an attempt to grow closed films where the interface layer is not

exposed, a thicker film was grown in three successive Mo deposition and oxidation steps ($3 \times 1.15 \text{ MLE Mo}$). This approach was tried here because it gave good results for V_2O_5 thin films on Au(111).² A LEED pattern of this film (Figure

11) exhibits much weaker diffraction spots related to the interface layer. They are actually only discernible when the

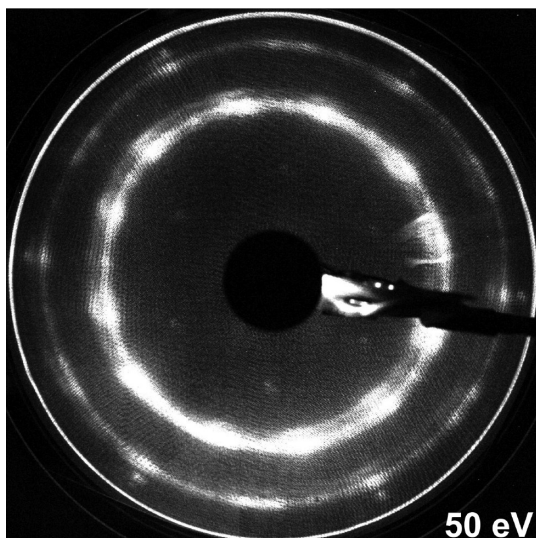


Figure 11. LEED pattern obtained for a film prepared by three successive steps of 1.15 MLE Mo deposition, followed by oxidation in 50 mbar O₂ at 673 K for 10 min (total of 3.45 MLE Mo).

contrast of the image is artificially enhanced (as was done in the case of Figure 11). It therefore seems possible to obtain smooth, well-ordered and closed MoO₃(010) films with this preparation method. Unfortunately, it was not possible to obtain any usable STM images for this film, probably because it was too thick.

A valence band photoemission spectrum acquired for a film grown from 2.3 MLE (~5 Å) Mo is shown in Figure 12. Its

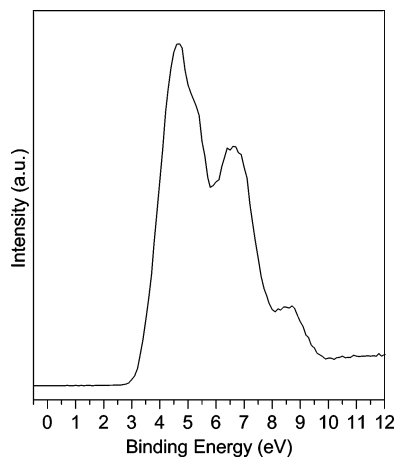


Figure 12. Valence band photoemission spectrum of a film prepared by oxidation of 2.3 MLE Mo on Au(111) in 50 mbar O₂ at 673 K for 10 min. The photon energy was 121 eV, and the electrons were detected at an exit angle of $\Theta = 70^\circ$ with respect to the surface normal.

intensity is dominated by O2sp contributions, with some admixture of Mo4d for the higher binding energy part.^{9,29} An increase in the Mo4d occupation typically results in a buildup of intensity between the Fermi edge and 3 eV.^{9,22,29} The absence of such intensity in Figure 12 is a strong indication that MoO₃(010) films prepared with the method used in this study exhibit very few oxygen vacancies.

Total yield Mo M_{2,3} and O K NEXAFS spectra of the film grown by oxidation of 2.3 MLE Mo are shown in Figure 13 for two different polar photon incidence angles. The spectra agree very well with those obtained for the (010) surface of MoO₃ single crystals,²⁹ and the angle-resolved O1s NEXAFS spectra calculated by Cavalleri and Hermann for the MoO₃(010) surface²⁸ correspond rather well to our results. The peaks below the ionization threshold (~537 eV) arise from O1s → O2p + Mo4d transitions; the features found at photon energies between 529 and 533 eV correspond to transitions into hybridized O2p(π) and Mo4d(t_{2g}) states (π^* orbitals perpendicular to the Mo–O bond), and the peaks at higher photon energies, between 533 and 536 eV, are due to transitions into hybridized O2p($\pi\sigma$) and Mo4d(e_{1g}) states (π^* orbitals along the Mo–O bond).^{28,29} The intensity variation of the various peaks as a function of the photon polar angle is predicted to be substantially different for the three types of oxygen centers contained in α -MoO₃.²⁸

Thermal Stability. The thermal stability of the MoO₃ layers under UHV conditions is a very important factor for reactivity studies because thermal reduction or sublimation of the catalyst may have a critical impact on catalytic reactions. For this reason, the stability of MoO₃(010)/Au(111) thin films was investigated with temperature-programmed desorption (TPD).

Figure 14 shows TPD curves obtained for a MoO₃(010) film prepared by oxidation of 3.45 MLE Mo. The evolution of the chamber pressure and the O₂ signal is shown in the lower graph, and the upper graph displays the most intense MoO_x signals, which correspond to MoO₂, MoO, and MoO₃ fragments. These species probably arise from the fragmentation of larger Mo_xO_y clusters in the ionizer of the quadrupole mass spectrometer. Indeed, detailed mass spectrometric studies revealed that Mo_xO_{3x} (with 3 ≤ x ≤ 5) aggregates are the primary products of the sublimation of MoO₃ in vacuum.³¹ The MoO_x desorption curves exhibit three features between 673 and 773 K: a rather broad peak centered at ~720 K, a sharp peak at 733 K, and some faint intensity between 743 and 773 K.

The overall appearance of the spectra is very similar to that observed for V₂O₅(001) layers on Au(111).² In that case, the broader peak at lower temperature was attributed to the sublimation of regular V₂O₅ and the sharp feature following this peak was assigned to desorption of the layers at the Au(111)–oxide interface. It may be reasonable to assume that this is similar for MoO₃ on Au(111). In this sense, the feature centered at 720 K might be attributed to the sublimation of the MoO₃(010) crystallites, whereas the other peaks observed at higher temperature are probably related to the interface layers.

For both oxides, V₂O₅(001)² and MoO₃(010), the result that the interface layer desorbs at higher temperature than the bulk-like structures may be explained by energy differences between the bonding of the interface layer to the Au(111) substrate and the interlayer adhesion energy: the layers (bilayers for MoO₃) in the bulk-like crystals interact via weak forces, whereas the interface layer might be bound more strongly to the substrate. Calculations for c(4 × 2) islands on Au(111)²⁶ indicate that there is an electronic interaction between the oxide and the Au(111), which balances the energy for the structural rearrangement of the oxide layer and which may also be responsible for a higher sublimation temperature.

In the case of V₂O₅(001) thin films,² oxide reduction (i.e., oxygen loss) was also observed. However, the O₂ TPD curve in Figure 14 does not show any defined desorption peak that could be clearly related to film reduction at temperatures up to

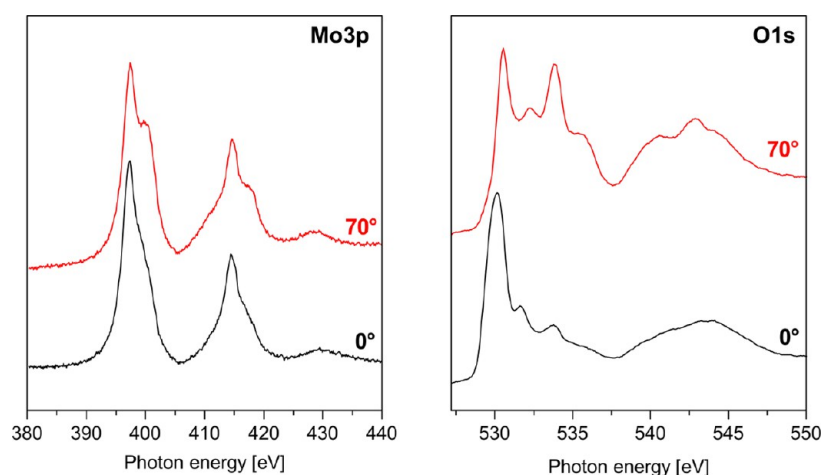


Figure 13. Total electron yield Mo3p (Mo $M_{2,3}$ edges) and O1s (O K-edge) NEXAFS spectra for a film prepared by oxidation of 2.3 MLE Mo/Au(111) in 50 mbar O_2 at 673 K for 10 min. Spectra for polar photon incidence angles of 0 and 70° are shown, 0° being along the surface normal.

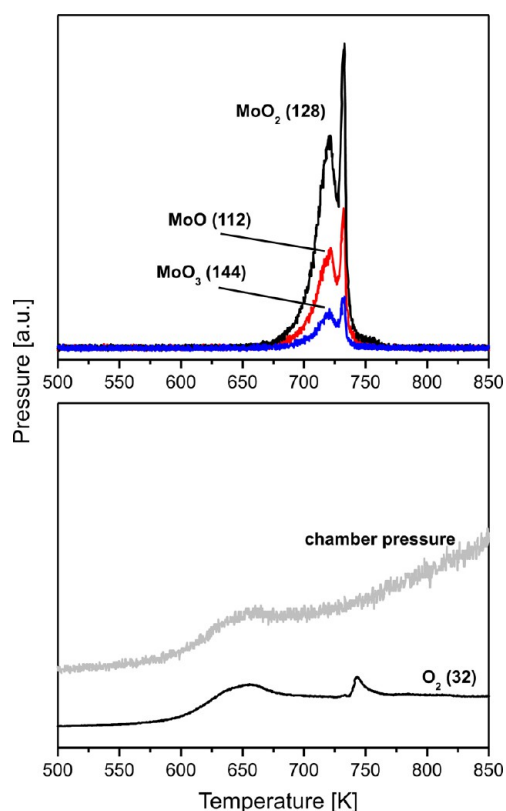


Figure 14. TPD spectra of a $MoO_3(010)$ film prepared by three successive steps of 1.15 MLE Mo deposition, followed by oxidation in 50 mbar O_2 at 673 K for 10 min (total of 3.45 MLE Mo). The evolution of the main chamber pressure during the TPD run is displayed in the lower graph. Numbers in brackets refer to the masses of the detected molecules.

~743 K. The broad O_2 desorption peak between 573 and 693 K is assigned to oxygen desorption from the platinum sample holder because this peak was observed in all V_2O_5 ² and MoO_3 TPD spectra. An O_2 desorption peak is clearly observed at 743 K in Figure 14. In the MoO_x desorption curves, the position of this O_2 peak coincides approximately with the beginning of the broad feature that follows the sharp peak. This O_2 desorption peak probably corresponds to the reduction of remaining MoO_3 in the monolayer regime. The thermal reduction of a

MoO_3 monolayer on Au(111) in UHV has been investigated by Deng and coworkers,³² who found that the reduction of the oxide $c(4 \times 2)$ overlayer occurs through the formation of extended 1D shear plane defects. Although they reported that the reduction occurs at ~648 K, they acknowledged that the actual temperature during their annealing experiment was probably higher because they also observed a partial oxide loss due to sublimation. No additional desorption features are observed above 773 K, and no traces of molybdenum or oxygen could be detected at the surface of the Au(111) substrate with XPS after TPD ramping up to 973 K. These observations apparently indicate that most of the film is evaporated after annealing up to 773 K in UHV.

SUMMARY

The results presented here show that well-ordered MoO_3 films can be formed on Au(111) by oxidation of molybdenum in 50 mbar of O_2 at elevated temperature. Oxidation of 0.46 MLE of Mo leads to the formation of a flat $c(4 \times 2)$ MoO_3 monolayer structure. The oxidation of 0.92 MLE of Mo results in MoO_3 bilayer films with a $11.6 \text{ \AA} \times 5 \text{ \AA}$ rectangular unit cell. These films are substrate-specific, and their structure is different from those of known bulk structures. Similar observations were made for V_2O_5 on Au(111).²⁷

Similar to the case of $V_2O_5(001)$ on Au(111),² $MoO_3(010)$ crystallites with random azimuthal orientation and very few point defects form for larger Mo coverages (observed for Mo coverages larger than 1.15 MLE). The films are apparently stable in UHV up to a temperature of ~673 K, above which $MoO_3(010)$ starts to sublime. These TDS data suggest that the substantial reduction does not occur until ~743 K.

AUTHOR INFORMATION

Corresponding Author

*E-mail: kuhlenbeck@fhi-berlin.mpg.de.

Present Addresses

[§]S. Guimond: OC Oerlikon Balzers AG, Iramali 18, LI-9496 Balzers, Liechtenstein.

^{||}D. Göbke: SUET Saat- and Erntetechnik GmbH, Sudetenlandstraße 26, 37269 Eschwege, Germany.

[†]J. M. Sturm: FOM-Institute for Plasma Physics Rijnhuizen, Postbus 1207, 3430 BE Nieuwegein, The Netherlands.

#M. Cavalleri: John Wiley & Sons, Inc., 111 River Street, Hoboken NJ 07030, USA.

Notes

The authors declare no competing financial interest.

ACKNOWLEDGMENTS

This work was funded by the Deutsche Forschungsgemeinschaft through their Sonderforschungsbereich 546 'Transition Metal Oxide Aggregates'. The Fonds der Chemischen Industrie is gratefully acknowledged for financial support. We acknowledge the Helmholtz-Zentrum Berlin – Electron storage ring BESSY II – for provision of synchrotron radiation at beamline UES2-PGM. M.C. thanks the AvH foundation for granting him a position as a postdoctoral research fellow at the Fritz-Haber-Institute.

REFERENCES

- (1) Biener, M. M.; Biener, J.; Schalek, R.; Friend, C. M. Growth of Nanocrystalline MoO₃ on Au(111) Studied by in Situ Scanning Tunneling Microscopy. *J. Chem. Phys.* **2004**, *121*, 12010–12016.
- (2) Guimond, S.; Sturm, J. M.; Göbke, D.; Romanyshyn, Y.; Naschitzki, M.; Kuhlbeck, H.; Freund, H.-J. Well-Ordered V₂O₅(001) Thin Films on Au(111): Growth and Thermal Stability. *J. Phys. Chem. C* **2008**, *112*, 11835–11846.
- (3) Hermann, K.; Witko, M. In *Oxide Surfaces*; King, D. A., Woodruff, D. P., Eds.; The Chemical Physics of Solid Surfaces; Elsevier: Amsterdam, The Netherlands, 2001; Vol. 9; pp 136–198.
- (4) Soares, A. P. V.; Portela, M. F.; Kiennemann, A. Methanol Selective Oxidation to Formaldehyde over Iron-Molybdate Catalysts. *Catal. Rev.* **2004**, *47*, 127–174.
- (5) Bowker, M.; Carley, A. F.; House, M. Contrasting the Behaviour of MoO₃ and MoO₂ for the Oxidation of Methanol. *Catal. Lett.* **2008**, *120*, 34–39.
- (6) Ressler, T.; Wienold, J.; Jentoft, R. E.; Girgsdies, F. Evolution of Defects in the Bulk Structure of MoO₃ During the Catalytic Oxidation of Propene. *Eur. J. Inorg. Chem.* **2003**, *2*, 301–312.
- (7) Kihlberg, L. Least Squares Refinement of the Crystal Structure of Molybdenum Trioxide. *Ark. Kemi* **1963**, *21*, 357–364.
- (8) Coquet, R.; Willock, D. J. The (010) Surface of α -MoO₃, a DFT + U Study. *Phys. Chem. Chem. Phys.* **2005**, *7*, 3819–3828.
- (9) Tokarz-Sobieraj, R.; Hermann, K.; Witko, M.; Blume, A.; Mestl, G.; Schlögl, R. Properties of Oxygen Sites at the MoO₃(010) Surface: Density Functional Theory Cluster Studies and Photoemission Experiments. *Surf. Sci.* **2001**, *489*, 107–125.
- (10) Smith, R. L.; Rohrer, G. S. The Protonation of MoO₃ during the Partial Oxidation of Alcohols. *J. Catal.* **1998**, *173*, 219–228.
- (11) Julien, C.; Khelifa, A.; Hussain, O. M.; Nazri, G. A. Synthesis and Characterization of Flash-Evaporated MoO₃ Thin Films. *J. Cryst. Growth* **1995**, *156*, 235–244.
- (12) Al-Kuhaili, M. F.; Durrani, S. M. A.; Khawaja, E. E. Effects of Preparation Conditions and Thermocoloration on the Optical Properties of Thin Films of Molybdenum Oxide. *Thin Solid Film* **2002**, *408*, 188–193.
- (13) Hussain, O. M.; Rao, K. S.; Madhuri, K. V.; Ramana, C. V.; Naidu, B. S.; Pai, S.; John, J.; Pinto, R. Growth and Characteristics of Reactive Pulsed Laser Deposited Molybdenum Trioxide Thin Films. *Appl. Phys. A: Mater. Sci. Process.* **2002**, *75*, 417–422.
- (14) Gaigneaux, E. M.; Fukui, K.-I.; Iwasawa, Y. Morphology of Crystalline α -MoO₃ Thin Films Spin-Coated on Si(100). *Thin Solid Films* **2000**, *374*, 49–58.
- (15) Bica de Moraes, M. A.; Trasferetti, B. C.; Rouxinol, F. P.; Landers, R.; Durrant, S. F.; Scarmio, J.; Urbano, A. Molybdenum Oxide Thin Films Obtained by the Hot-Filament Metal Oxide Deposition Technique. *Chem. Mater.* **2004**, *16*, 513–520.
- (16) Smudde, G. H., Jr.; Stair, P. C. The Oxidation of Mo(100) Studied by XPS and Surface Raman Spectroscopy: the Onset of MoO₂

Formation and the Formation of Surface Polymolybdate. *Surf. Sci.* **1994**, *317*, 65–72.

(17) Zhang, C.; van Hove, M. A.; Somorjai, G. A. The Interaction of Oxygen with the Mo(100) and Mo(111) Single-Crystal Surfaces: Chemisorption and Oxidation at High Temperatures. *Surf. Sci.* **1985**, *149*, 326–340.

(18) Schroeder, T.; Zegenhagen, J.; Magg, N.; Immaraporn, B.; Freund, H. J. Formation of a Faceted MoO₂ Epilayer on Mo(112) Studied by XPS, UPS and STM. *Surf. Sci.* **2004**, *552*, 85–97.

(19) Radican, K.; Berdunov, N.; Manai, G.; Shvets, I. V. Epitaxial Molybdenum Oxide Grown on Mo(110): LEED, STM, and Density Functional Theory Calculations. *Phys. Rev. B* **2007**, *75*, 155434.

(20) Petukhov, M.; Rizzi, G. A.; Domenichini, B.; Granozzi, G.; Bourgeois, S. Scanning Tunneling Microscopy and Spectroscopy of Mo Clusters Grown on TiO₂(110). *Surf. Sci.* **2007**, *601*, 3881–3885.

(21) Feulner, P.; Menzel, D. Simple Ways to Improve Flash Desorption Measurements from Single Crystal Surfaces. *J. Vac. Sci. Technol.* **1980**, *17*, 662–663.

(22) Werfel, F.; Minni, E. Photoemission Study of the Electronic Structure of Mo and Mo Oxides. *J. Phys. C: Solid State Physics* **1983**, *16*, 6091–6100.

(23) Saburi, T.; Murata, H.; Suzuki, T.; Fujii, Y.; Kiuchi, K. Oxygen Plasma Interactions with Molybdenum: Formation of Volatile Molybdenum Oxides. *J. Plasma Fusion Res.* **2002**, *78*, 3–4.

(24) Holland, B. W.; Woodruff, D. P. Missing Spots in Low Energy Electron Diffraction. *Surf. Sci.* **1973**, *36*, 488–493.

(25) Biener, M. M.; Friend, C. M. Heteroepitaxial Growth of Novel MoO₃ Nanostructures on Au(111). *Surf. Sci.* **2004**, *559*, L173–L179.

(26) Quek, S. Y.; Biener, M. M.; Biener, J.; Friend, C. M.; Kaxiras, E. Tuning Electronic Properties of Novel Metal Oxide Nanocrystals Using Interface Interactions: MoO₃ Monolayers on Au(111). *Surf. Sci.* **2005**, *577*, L71–L77.

(27) Guimond, S.; Göbke, D.; Romanyshyn, Y.; Sturm, J. M.; Naschitzki, M.; Kuhlbeck, H.; Freund, H.-J. Growth and Characterization of Ultrathin V₂O₅ ($y \approx 5$) Films on Au(111). *J. Phys. Chem. C* **2008**, *112*, 12363–12373.

(28) Cavalleri, M.; Hermann, K.; Guimond, S.; Romanyshyn, Y.; Kuhlbeck, H.; Freund, H.-J. X-Ray Spectroscopic Fingerprints of Reactive Oxygen Sites at the MoO₃(010) Surface. *Catal. Today* **2007**, *124*, 21–27.

(29) Sing, M.; Neudert, R.; von Lips, H.; Golden, M. S.; Knupfer, M.; Fink, J.; Claessen, R.; Mücke, J.; Schmitt, H.; Hüfner, S.; et al. Electronic Structure of Metallic K_{0.3}MoO₃ and Insulating MoO₃ from High-Energy Spectroscopy. *Phys. Rev. B* **1999**, *60*, 8559–8568.

(30) Smith, R. L.; Rohrer, G. S. Scanning Probe Microscopy of Cleaved Molybdates: α -MoO₃(010), Mo₁₈O₅₂(100), Mo₈O₂₃(010), and η -Mo₄O₁₁(100). *J. Solid State Chem.* **1996**, *124*, 104–115.

(31) Fialko, E. F.; Kikhtenko, A. V.; Goncharov, V. B.; Zamaraev, K. I. Molybdenum Oxide Cluster Ions in the Gas Phase: Structure and Reactivity with Small Molecules. *J. Phys. Chem. A* **1997**, *101*, 8607–8613.

(32) Deng, X.; Quek, S. Y.; Biener, M. M.; Biener, J.; Kang, D. H.; Schalek, R.; Kaxiras, E.; Friend, C. M. Selective Thermal Reduction of Single-Layer MoO₃ Nanostructures on Au(111). *Surf. Sci.* **2008**, *602*, 1166–1174.